

Logarithmic corrections to scaling in turbulent thermal convection

B. Dubrulle^{1,2}

¹ *CNRS, Service d'Astrophysique, CE Saclay, F-91191 Gif sur Yvette Cedex, France*

² *CNRS, URA 285, Observatoire Midi-Pyrénées, 14 avenue Belin, F- 31400 Toulouse, France*

Abstract

We use an analytic toy model of turbulent convection to show that most of the scaling regimes are spoiled by logarithmic corrections, in a way consistent with the most accurate experimental measurements available nowadays. This sets a need for the search of new measurable quantities which are less prone to dimensional theories.

47.27 -i Turbulent flows, convection and heat transfer

47.27.Eq Turbulence simulation and modeling

47.27.Te Convection and heat transfer

When an horizontal layer of fluid is heated from below, a heat exchange from the bottom to the top layer occurs. Dimensional consideration show that the non-dimensional heat exchange Nu depends on the geometry (via for example the aspect ratio), on the boundary conditions, and on the Rayleigh Ra and the Prandtl number Pr . Further dimensional analysis of the dynamical equations governing the convective layer suggests that this dependence be a power-law. The exponent of the power law depends on the (dimensional) basic hypothesis. The classical theory predicts that $Nu \sim Ra^\beta$ with $\beta = 0.33$, which seems to be observed in electro-chemical convection [1]. Other theories lead to $\beta = 0.2$ or 0.24 [2], $\beta = 2/7$ [3,4] or $\beta = 1/2$ [5] depending on the regime considered. A unifying synthesis of the possible scaling regimes, including their Prandtl dependence has been recently made by Grossman and Lohse [6,7]. From the experimental point of view, the situation is rather unclear, since almost all the range of exponents between 0.25 and 0.33 has been measured (see [6] for a recent detailed review of the experimental measurements). Furthermore, recent experiments with fluids subject large variation of the Prandtl number have led to a new exploration of the phase parameter, and uncovered new scaling laws as a function of the Prandtl number. This new exploration can be used as a stringent tool to discriminate between the various theories, since two competing theories can provide the same value of β , but different Prandtl number dependence.

On the other hand, it is not quite clear whether the present dimensional theories satisfactorily capture the dependence of Nu as a function of Pr and Ra . In a recent serie of experiments, conducted with acetone at various aspect ratio, [8] show that their measurements are inconsistent with a single power law $Nu(Ra)$, because the local effective exponent $\beta_{eff} = d \ln Nu / d \ln Ra$ varies continuously with Ra in the range of Rayleigh number they consider. This effect can easily be accounted for in the scaling theory by considering a superposition of scaling laws, as proposed by [6]. There is another solution, connected with the

existence of logarithmic corrections to scalings (see e.g. [4]). The difficulty associated with such a solution is that logarithmic corrections cannot be uncovered by dimensional analysis (nor numerical simulations!), and require detailed analytical computations. At the present time, there are no available analytical solutions of the full Boussinesq equations describing the dynamics of the convective motions, in the turbulent regime. Some time ago, Malkus [9] proposed to combine a weakly non-linear theory past the critical point, combined with a maximum principle to obtain approximate analytical solutions of the full problem. This approach developed further by Howard, Roberts, Stewartson and Herring (see refs [10] for a summary) gives $Nu = 0.24(Ra \ln Ra)^{3/10}$. Such a law with logarithmic correction fits the recent experimental data by Niemela et al. [11] very well.

In the present work, we explore the predictions obtained using a solvable model of turbulent convection. This model couples large scale mean sheared velocity and temperature fields $U = (U(z), 0, 0)$ and $\Theta(z)$, with small scale random velocity and temperature fields. This kind of large scale geometry is generally accepted as representative of the Boussinesq convection in the boundary layers, due to the shearing effect of the large convective cells. The model is closed by deriving an equation for the random component from the Boussinesq equation using two simplifying assumptions: i) the non-linear interactions of the small scale scales between themselves is modeled via a turbulent viscosity; ii) the small scale generation via the breaking of large scale structures is modeled by a random small scale forcing with prescribed statistics. This results in a linear stochastic equation for the random small scales, which can be analytically solved in the shear flow geometry by a decomposition of the small waves into localized wave-packets. In [12,13], the solution of the turbulent model were computed in the restricted case of 2D geometry, and turbulent Prandtl number equal to unity. This leads to expression of the mean and fluctuating velocity and temperature profile, as a function of Nu , Ra and Pr . In [13], these results were combined with dimensional estimates to derive the scaling laws governing the transport of heat. In the present contribution, we proceed one step further and use the analytical predictions about the profiles to compute directly the heat and energy dissipated across the turbulent boundary layer. From this, we derive an analytical expression of the non-dimensional heat flux, as a function of Pr and Ra .

There can be a debate about whether such a simple model correctly accounts for the complex dynamics of the full, turbulent Boussinesq equations. A systematic numerical check of the various hypotheses pertaining the model has been undertaken in the past years [14] and is still underway. In any case, we think that this model is very illustrative as to what kind of mechanism could take place in real, turbulent convection. Our computations show that most of the likely scaling regimes are spoiled by logarithmic corrections, in a way consistent with the most accurate experimental measurements available nowadays. We believe that this sets a need for the search of new measurable quantities which are less prone to dimensional theories.

To set up notations, we start by a brief summary of the turbulent model [12,13] and of results obtained within it. In this model, the dynamics of the turbulent boundary layer is obtained from solutions of two coupled sets of equations. The first one described the dynamics of the mean (shear like) velocity $\mathbf{U} = \langle \mathbf{u} \rangle = (U(z), 0, 0)$ and temperature $\Theta(z) = \langle \theta \rangle$:

$$\begin{aligned} \partial_t U + \partial_z \langle u'w' \rangle &= -\partial_x P + Pr \partial_z^2 U, \\ \partial_t \Theta + \partial_z \langle w'\theta' \rangle &= \partial_z^2 \Theta. \end{aligned} \tag{1}$$

These equations have been expressed, following [4] in units the thermal diffusivity and the cell height. Here, Pr is the Prandtl number, the primes denote fluctuating (small scale) quantities and $\langle \rangle$ the averaging. In the stationary case, we get from (1) that $\partial_x P$ is a constant, independent of z . In the laminar case where $\langle u'w' \rangle$ and $\langle w'\theta' \rangle$ are negligible, we thus obtain the well known parabolic profile for the velocity and the linear profile for the temperature. In the turbulent case, the profiles are linear within the thermal or the viscous layer, while outside this layer, they are given by the condition

$$\partial_z \langle u'w' \rangle = -\partial_x P, \quad \partial_z \langle w'\theta' \rangle = 0. \quad (2)$$

To close the system, we need $\langle u'w' \rangle$ and $\langle w'\theta' \rangle$. They are obtained as solution of a linear, stochastic equation valid for localized wave-packets of velocity and temperature:

$$\begin{aligned} D_t \hat{u}_i &= -ik_i \hat{p} - \hat{w} \partial_z U \delta_{i1} + Ra Pr \hat{\theta} \delta_{i3} - Pr^t \mathbf{k}^2 \hat{u}_i + \hat{f}_i^{(u)} \\ D_t \hat{\theta} &= -\hat{w} \partial_z \Theta - \mathbf{k}^2 \hat{\theta} + \hat{f}^{(\theta)}, \end{aligned} \quad (3)$$

where

$$\hat{u}(\mathbf{x}, \mathbf{k}, t) = \int g(|\mathbf{x} - \mathbf{x}'|) e^{i\mathbf{k} \cdot (\mathbf{x} - \mathbf{x}')} \mathbf{u}(\mathbf{x}', t) d\mathbf{x}', \quad (4)$$

g being a function which decreases rapidly at infinity. We have dropped primes on fluctuating quantities for convenient notations and introduced the total derivative $D_t = \partial_t + U \partial_x - \partial_z (U k_x) \partial_{k_z}$. Note that the linear part of (3) is exact and describes the non-local interactions between the mean and the fluctuating part. The major approximation of the model is to lump the non-linear terms describing local interactions between fluctuations into a turbulent viscosity, or equivalently, into a turbulent Prandtl number Pr^t . The forces $f^{(u)}$ and $f^{(\theta)}$ appearing in (3) are small scale random forces which are introduced to model the seeding of small scales by energy cascades (for example via turbulent plumes, detaching from the wall).

The analytical solutions of (1) and (3) have been obtained in [12,13] in the 2D case (no movement in the direction transverse to the mean flow), and for $Pr^t = 1$. There are numerical and analytical evidence that 2D geometry is sufficient to capture the physical mechanism responsible for the Nu scaling with Ra [15] and also to capture the correct shape of the equilibrium profile in the neutral case [16]. Note that the vortex stretching, which is theoretically absent in 2D geometry, has been implicitly accounted for via the turbulent viscosity. The unit value of Pr^t was dictated by our ignorance of the exact value of this parameter (which is likely to depend on Pr). We shall keep in mind that it may induce a wrong dependence of the correlations with respect to the Prandtl number. In any case, we shall consider these solutions as a toy model of turbulent thermal convection, and investigate their scaling properties. For the mean flows, the solution are [13]:

$$\partial_z U \sim \frac{1}{z}, \quad \partial_z \Theta \sim \frac{1}{z^2}, \quad (5)$$

resulting in a constant (with z) Richardson number:

$$R_i = Ra Pr \frac{\partial_z \Theta}{(\partial_z U)^2}. \quad (6)$$

In developed convective turbulence, this number is large and negative $Ri \ll -1$. This motivates a large Ri expansion of the solution of (3), which provides the expression of the correlations as :

$$\begin{aligned}
\langle w'u' \rangle &\approx \frac{u_*^2}{\partial_z U} \propto z, \\
\langle w'\theta' \rangle &\approx \frac{u_*^2 \sqrt{-Ri}}{RaPr} \propto cte = Nu, \\
\langle w'^2 \rangle &\approx \frac{u_*^2}{\partial_z U}, \\
\langle \theta'^2 \rangle &\approx Ri \frac{u_*^2 \partial_z U}{(RaPr)^2} = \frac{u_*^2 \partial_z \Theta}{RaPr \partial_z U}.
\end{aligned} \tag{7}$$

where we have introduced $u_*^2 = (\partial_z U / k_*^2)^{2\sqrt{-Ri}/3}$. Note that the last equation of (7) just reflects the balance between the vertical energy and the buoyancy force. Such a balance can be expected to hold only at $Pr > 1$ [2]. For low Pr , temperature fluctuations were found to behave like a passive scalar, except in the boundary layers, or in the center of the cell [17]. Since our expression pertain only to the boundary layers, we feel safe to consider it for both the $Pr > 1$ and the $Pr < 1$ regime.

The second equation of (7) can be used to express u_* as a function of Nu and Ri . Then, we can eliminate Ri by matching the turbulent profiles with the viscous or diffusive solutions $Pr \partial_z U = u_\tau^2$ and $\partial_z \Theta = Nu$, where u_τ is the friction velocity and Nu the Nusselt number. For this, we introduce the thermal length scale $\lambda_\theta = 1/2Nu$ and the viscous length scale $\lambda_u = KPr/u_\tau$ ($K \approx 0.4$ is the Karman constant), and operate the matching via smooth functions according to:

$$\begin{aligned}
\partial_z U &= \frac{u_\tau^2 Pr^{-1}}{\sqrt{1 + (z/\lambda_u)^2}}, \\
\partial_z \Theta &= \frac{Nu}{1 + (z/\lambda_\theta)^2}.
\end{aligned} \tag{8}$$

The shape of $\partial_z U$ is dictated by the exact analytical solutions of the profile found by [16] in a neutral layer. The shape of $\partial_z \Theta$ was chosen as the simplest smooth function matching the viscous and turbulent layers. Using these expressions, we can eliminate Ri and write for the fluctuations:

$$\begin{aligned}
\langle w'^2 \rangle &= Nu^{3/2} (RaPr)^{1/2} \frac{u_\tau}{\partial_z U}, \\
&= Nu^{3/2} (RaPr)^{1/2} \frac{Pr}{u_\tau} \sqrt{1 + (z/\lambda_u)^2}, \\
\langle \theta'^2 \rangle &= u_\tau \frac{Nu^{3/2}}{(RaPr)^{1/2}} \frac{\partial_z \Theta}{\partial_z U} \\
&= \frac{Pr}{u_\tau} \frac{Nu^{5/2}}{(RaPr)^{1/2}} \frac{\sqrt{1 + (z/\lambda_u)^2}}{1 + (z/\lambda_\theta)^2}.
\end{aligned} \tag{9}$$

Note that these fluctuations exist only for $z > \lambda_u$. The expression we derived are only valid inside the turbulent layers, which we define as the locations where the fluctuations of

horizontal velocity and of temperature reach a maximum. The scales at which these maxima are reached are labeled λ_{BLV} and λ_{BLT} , respectively. Beyond these scales, the flow enters the "bulk region", in which the velocity and temperature fields are organized into convective large scale, whose details are non-universal and strongly depend on the geometry (aspect ratio) of the cell. It is difficult to evaluate analytically the vertical dependence of the profiles. On the other hand, support from data can only be provided by numerical simulations, encompassing relatively low Rayleigh numbers. One important outcome of these simulations [18–20] is the existence of two distinct flow regimes: one for $Pr < 0.35$ in which the flow is dominated by a large re-circulation cell, and one $Pr > 0.35$ in which isolated thermal plumes can develop. The detailed scaling of the velocity pattern has only been partially studied by Kerr [21] in the regime $Pr = 0.7$, $Ra = 8 \times 10^7$ and for aspect ratio 1. He found no indication of the logarithmic region, but rather a variation of the horizontal velocity profile consistent with a $z^{-1/2}$ law. This can be easily understood by noting first, that in this Prandtl regime, the Reynolds number corresponding to $Ra = 8 \times 10^7$ is too low to allow for a well developed turbulent boundary layer. Therefore, the logarithmic region is non-detectable. On the other hand, in the core, there is a tendency for strongly homogeneous temperature (due perhaps to the presence of plumes, which favor the good mixing), with nearly constant value Θ_0 throughout the central region. The classical free fall velocity argument then predicts vertical velocities varying like $W^2 \sim RaPr\Theta_0z$, resulting, by incompressibility $\partial_z U \sim \partial_z W$ in a $z^{-1/2}$ law for the horizontal profile. Given the small extent of the logarithmic zone in this regime, we shall therefore approximate the bulk velocity in this region, at $Pr > 0.35$ by $u_\tau(z/\lambda_u)^{-1/2}$ (to ensure the matching with the viscous layer). Unfortunately, no comparable measurements are available at low Pr. On the one hand, we can expect the logarithmic region to be more extended in this regime, because of the larger Reynolds number involved. Interestingly enough, inversion of the temperature profiles in the central region have been detected in the experiment of [17], with a nearly constant and positive value of dT/dz (whether this is correlated with the absence of plumes is an interesting open question). In such a case, the free-fall argument (which is valid provided we are in the Bolgiano regime, i.e. at large enough scales) predicts vertical velocities varying like $W^2 \sim RaPrz^2$, i.e., via the incompressibility, constant horizontal velocity profiles. Flatter profiles of horizontal velocity have indeed been observed in some numerical simulations of Kerr [21], but the scaling has not been properly checked. In any case, as a first approximation, we shall assume that the horizontal velocity in the central region and in the $Pr < 0.35$ regime, is constant U_0 . The matching of this constant with the logarithmic profile then imposes $U_0 = Ku_\tau(\ln(\lambda_o) + B)$, where λ_o is the outer scale, and B is a constant which may depend on the Prandtl number (under neutral condition, $B \approx 5$). In the sequel, we assume $U_0 = fu_\tau$, and assume that f is independent of the Prandtl number (for $Pr < 0.35$).

These estimates can be further used to determine the scaling behaviors of the two scales λ_{BLT} and λ_{BLV} characterizing the turbulent boundary layer. For this, we follow the logic of our turbulent model which states that in the boundary layer, the fluctuations are passively advected by the large scale horizontal velocity and obeys $U\partial_x u' = Pr\partial_z^2 u'$ or $U\partial_x \theta' = \partial_z^2 \theta'$. On dimensional ground, this shows that the two scales are determined via the two implicit equations:

$$U(\lambda_{BLT}) \sim \frac{1}{\lambda_{BLT}^2}, \quad U(\lambda_{BLV}) \sim \frac{Pr}{\lambda_{BLV}^2}. \quad (10)$$

Here, we have ignored the aspect ratio dependence. Aspect ratio obviously affects the scaling regimes, but since we cannot quantify its effect in the large scale circulation, we shall ignore it hereafter. Depending on the Reynolds number $Re = u_\tau/Pr$ and on the Prandtl number, different regimes of velocity will be probed by this implicit relations, and the scaling of λ_{BLV} and λ_{BLT} as a function of Pr and u_τ will vary. Introducing $\epsilon(\lambda) = d \ln U / d \ln z|_{z=\lambda}$ (where $\lambda = \lambda_{BLV}$ or λ_{BLT}), we can summarize this dependence as:

$$\begin{aligned}\lambda_{BLT} &= Pr^{\epsilon/(2+\epsilon)} u_\tau^{-(1+\epsilon)/(2+\epsilon)} \left(\frac{1}{\ln \lambda_{BLT}} + \frac{1}{f} \right)^{\delta(\epsilon)/(2+\epsilon)}, \\ \lambda_{BLV} &= \left(\frac{Pr}{u_\tau} \right)^{(1+\epsilon)/(2+\epsilon)} \left(\frac{1}{\ln \lambda_{BLV}} + \frac{1}{f} \right)^{\delta(\epsilon)/(2+\epsilon)}.\end{aligned}\quad (11)$$

Here, $\delta(\epsilon)$ is equal to 1 if $\epsilon = 0$ and zero elsewhere. The dependence of ϵ in λ_{BLT} and λ_{BLV} has been omitted for simpler notations. Also, the logarithmic and constant velocity regime have been lumped into the single notation $U(\lambda) \sim u_\tau/(1/\ln \lambda + 1/f)$ which patches the two consecutive characteristic behaviors.

These considerations can be used to compute the Rayleigh and Prandtl dependence of the Nusselt number. For this, we follow [4,6] and use the two rigorous relations involving the global average of the kinetic and thermal dissipation rates:

$$\begin{aligned}\langle Pr(\partial_i u_j)^2 \rangle_V &= Ra Pr (Nu - 1), \\ \langle (\partial_i \theta)^2 \rangle_V &= Nu.\end{aligned}\quad (12)$$

In (12) averages are taken over spatial volumes. Dissipation takes place both in the boundary layers, and in the "bulk" region. However, several independent observations militates in favor of the importance of boundary layers, rather than bulk region, to determine the scaling of the Nusselt with the Rayleigh number. For example, Julien et al [22] observe that when switching from no-slip to stress-free boundary conditions, the exponent of the power-law Nusselt versus Rayleigh changes from close to 2/7 to close to 1/3. More recently, Ciliberto and Laroche [23] observed that both the prefactor and the exponent of the power-law changes when switching from smooth to rough bottom plate in the convective cell. On the other hand, blocking the large scale circulation does not affect the heat transport [24]. In numerical simulations at $Pr = 0.7$ and $Ra = 8 \times 10^7$, Kerr [21] noted that a change of aspect ratio (which changes the large scale circulation) only affects the energy dissipation in the bulk of the flow. In the boundary layers, the total dissipation seems to remain always about 1/4 of the total dissipation. Gathering all these information, we shall assume that a constant fraction of heat and energy is dissipated in the boundary layers, independently of geometry, Rayleigh number, Prandtl number... This allow us to consider similar equations to (12), where the average is only taken over the volume encompassed by the boundary layers. The advantage is that, in that region, we can use our exact analytical solutions to compute the kinetic and thermal dissipation.

In each case, these dissipation include two contributions: one from the mean flow, and one from the fluctuations. For the mean flow contribution, we use (8) and find:

$$\epsilon_U = Pr \int_0^{\lambda_{BLV}} dz (\partial_z U)^2 = Ku_\tau^3 \text{arctg} \left(\frac{\lambda_{BLT}}{\lambda_u} \right),$$

$$\epsilon_{\Theta} = \int_0^{\lambda_{BLT}} dz (\partial_z \Theta)^2 = \frac{Nu^2}{2\lambda_{\theta}} \left[\frac{\lambda_{BLT}/\lambda_{\theta}}{1 + (\lambda_{BLT}/\lambda_{\theta})^2} + \arctg \left(\frac{\lambda_{BLT}}{\lambda_{\theta}} \right) \right]. \quad (13)$$

For the fluctuations, we first note that the velocity and thermal fluctuations are non-negligible only for $z > \lambda_u$ ¹. Further, we use incompressibility to get $(\partial_z u)^2 \sim \lambda_{BLV}^{-2} (\partial_x u)^2 \sim \lambda_{BLV}^{-2} (\partial_z w)^2$. Then, we approximate $\partial_z w \sim \partial_z \sqrt{\langle w^2 \rangle}$ and $\partial_z \theta \sim \partial_z \sqrt{\langle \theta^2 \rangle}$. Using (9) and performing the integration, we finally obtain for the contribution of the fluctuations:

$$\begin{aligned} \epsilon_u &\sim \frac{(NuPr)^{3/2} Ra^{1/2}}{4K} \left(\frac{1}{2} - \frac{(\lambda_{BLV}/\lambda_u)}{\sqrt{1 + (\lambda_{BLV}/\lambda_u)^2}} + \ln \left(\frac{2\sqrt{1 + (\lambda_{BLV}/\lambda_u)^2} + 2(\lambda_{BLV}/\lambda_u)}{2\sqrt{2} + 2} \right) \right), \\ \epsilon_{\theta} &\sim \frac{Nu^{5/2}}{4K(RaPr)^{1/2}} \int_1^{\lambda_{BLT}/\lambda_u} dx \frac{x^2(1 + 2\eta - \eta^2 x^2)^2}{(1 + x^2)^{3/2}(1 + \eta^2 x^2)^3}, \quad \eta = \lambda_u/\lambda_{\theta}. \end{aligned} \quad (14)$$

Based on these expressions, we can singularize six different regimes. In the first three regimes, the dissipation is dominated by the mean flow contribution. This regimes are expected to hold at low Reynolds number (the turbulence is weak) or when the Prandtl number is low, according to the numerical study of [18]. The thermal dissipation then fixes $\lambda_{BLT} \sim Nu^{-1}$. Then we can distinguish two cases: at very low Reynolds number, the boundaries are non-turbulent, and we have $\lambda_{BLV} < \lambda_u$, so that $\epsilon_U \sim u_{\tau}^4 \lambda_{BLV}/Pr$, and the two boundary layer scales follow (11) with $\epsilon = 1$. In this regime, we get:

$$Nu \sim Ra^{1/4} Pr^{-1/12}, \quad Re \sim Ra^{3/8} Pr^{-5/8}. \quad (15)$$

This Nusselt versus Rayleigh dependence corresponds to regime I_u of [6]. They argue that for fixed Raleigh number, it could explain the weak decrease of the Nusselt number observed at large Prandtl number. For larger Reynolds number, when $\lambda_{BLT} > \lambda_u$, we get to a regime where $\epsilon_U \sim u_{\tau}^3 \sim RaPrNu$. This corresponds to a Reynolds number varying like $(RaNu)^{1/3}$, a situation observed in the low Prandtl number experiment of [2]. The final expression of Nu depends on how the thermal boundary layer scale $\lambda_{BLT} \sim Nu^{-1}$ varies with the mean flow. Using (11), we obtain:

$$Nu \sim \frac{Ra^{(1+\epsilon)/(5+2\epsilon)} Pr^{(1-2\epsilon)/(5+2\epsilon)}}{(1/\ln(Nu) + 1/f)^{3\delta(\epsilon)/(5+2\epsilon)}}. \quad (16)$$

For $\epsilon \sim 1$ (which may be obtained at low Rayleigh, for $Pr > 0.35$), this corresponds to the 2/7 law of [4], in which the Nusselt decreases like $Pr^{-1/7}$ and the Reynolds number varies like $Ra^{-3/7}$. For low Prandtl, we have to consider the case $\epsilon = 0$. In that case, we observe an interesting regime, where the Nusselt varies like $Ra^{1/5}(\ln Ra)^{3/5}$ at moderate Ra, then turning into a $Ra^{1/5}$ regime for larger Ra. The logarithmic correction increases the scaling exponent up to a value close to 1/4, as shown in Fig. 1. In this regime, experimental measurements will tend to show first a 1/4 regime, followed by transition to a 1/5 regime,

¹Temperature fluctuations are generated through velocity fluctuations, and, thus, are slaved to them

when the logarithmic corrections vanish, i.e. when the scaling of the boundary layer scale is determined by the bulk flow. This regime therefore exactly explain the experiments by [2].

Other interesting regimes appear when the fluctuations dominate the kinetic or thermal dissipation. The conditions under which this situation appears cannot be determined by a mere estimate of the ratio of ϵ_u versus ϵ_U , for example, because there are some indications that this condition is in fact subject to boundary conditions. For example, experiments conducted at same aspect ratio, same cylindrical geometry and same Prandtl number by [2] and [25] lead to different values of the Nusselt number. In [2], the scaling relation $Re \sim (RaNu)^{1/3}$ (characterizing the regime in which kinetic energy dissipation is dominated by the mean flow) is satisfied. In the experiment of [25], a careful study of the length scales revealed a significant deviation from the law $\lambda_{BLT} \sim 1/Nu$ which would be obtained in the regime explaining the experiment by [2], and in which the thermal dissipation is provided by the mean temperature profile. It is then logical to attribute the difference of Nusselt via a difference in boundary conditions, which would favor or not the dominance of fluctuations. For example, the thickness or composition of the bottom plate may play such a role (Castaing, private communication).

Let us consider first the regime in which mean flow dominates the thermal dissipation, but fluctuations dominates the kinetic dissipation. In such a case, we still have $\lambda_{BLT} \sim 1/Nu$, but the scaling of Nu depends on the behavior of λ_{BLV} . Assuming (11), and taking $\epsilon = 1$ for λ_{BLT} (no fluctuations of temperature), we get:

$$Nu \sim \frac{Ra^{(2+\epsilon)/(8+7\epsilon)} Pr^{\epsilon/(8+7\epsilon)} [\ln(\lambda_{BLV}/\lambda_u)]^{-2(2+\epsilon)/(8+7\epsilon)}}{(1/\ln(\lambda_{BLV}) + 1/f)^{-4\delta(\epsilon)/(8+7\epsilon)}}. \quad (17)$$

For $\epsilon = -1/2$ (valid for $Pr > 0.35$), we obtain two different behaviour with (17): one, with $\lambda_{BLV}/\lambda_u \approx 1$. This situation prevails for example under stress-free boundary conditions, like studied by WernePC, or for very large aspect ratio. It may also occur at very large Prandtl number, if, as discussed in [6] the viscous length scale approaches the size of the box and cannot increase any further. In such situation, we get $Nu = Ra^{1/3} Pr^{-1/9}$. In the opposite situation, where $\lambda_{BLV}/\lambda_u \gg 1$, we then have (within logarithmic corrections) $\lambda_{BLV} \sim Re^{1/3}$. This gives $Nu \sim Ra^{1/3}/(\ln(Ra))^{2/3}$. This law reproduces extremely well the recent experimental measurement of Niemela et al. [11], obtained with Helium ($Pr = 0.7$) over 11 decades of Rayleigh numbers. These measurements can be fitted by a power-law with exponent 0.308 over this range of Rayleigh number. However, as shown in Figure 2., even over such a wide range, the law with logarithmic corrections cannot be distinguished from the power-law exponent. Other measurements are also explained by this regime, for $Pr > 0.35$. For example, in this regime, we predict a variation of the Nusselt number with the Prandtl number going like $Nu \sim Pr^{-1/9}/\ln(Pr)$ (because Re depends on the Prandtl number). This variation is shown in Figure. 3. A power-law fit of this variation over $0.7 < Pr < 100$ gives an exponent -0.2 , exactly like in the experiment of Ashkenazi and Steinberg [26]. Also, the Reynolds number in this regime varies like $Re = \sqrt{Nu^3/Pr}$. The power-law dependence mimicked by the logarithmic corrections is (see Fig. 4 and 5) $Re \sim Ra^{0.46} Pr^{-0.8}$, again, in excellent agreement with the measurement of [26]. Other quantities, like the scaling of the central fluctuating temperature, or the length scales (Table IV) are also in excellent agreement with direct measurements of Niemela et al. [11] or by Kerr [19]. We do not discuss the regime corresponding to $\epsilon = 0$ in (17) because, apparently, it is not applicable to the low

Prandtl regime: it assumes that $\lambda_{BLT} < \lambda_u$, at variances with experimental observations by Segawa et al [17].

The last regime is obtained when temperature fluctuations dominate the thermal dissipation, making λ_{BLT} differ from $1/Nu$. The two interesting regimes then depend on whether $\eta = \lambda_u/\lambda_\theta = Nu/Re$ is less or larger than 1. In the first case, we get:

$$\begin{aligned}\epsilon_\theta &\sim \frac{Nu^{5/2}}{4K(RaPr)^{1/2}} \int_1^{\lambda_{BLT}/\lambda_u} dx \frac{x^2}{(1+x^2)^{3/2}} \\ &\sim \frac{Nu^{5/2}}{4K(RaPr)^{1/2}} \ln(\lambda_{BLT}/\lambda_u).\end{aligned}\quad (18)$$

We then get from (12) that $Nu \sim (RaPr)^{1/3}/(\ln(\lambda_{BLT}/\lambda_u))^{2/3}$. This regime is similar to regime (17), with a different prefactor. In the case where $\eta \gg 1$, we get

$$\begin{aligned}\epsilon_\theta &\sim \frac{Nu^{5/2}}{4K(RaPr)^{1/2}} \int_1^{\lambda_{BLT}/\lambda_u} \frac{dx}{\eta^2 x^2} \\ &\sim \frac{Nu^{1/2} u_\tau^2}{4K(RaPr)^{1/2}}.\end{aligned}\quad (19)$$

From (12), we get $Re = u_\tau/Pr = Pr^{-3/4}(RaNu)^{1/4}$. Using the expression (11) for λ_{BLV} , and $\epsilon_u = RaPrNu$, we finally get :

$$Nu \sim \frac{Ra^{1/(3+2\epsilon)} Pr^{(1+2\epsilon)/(3+2\epsilon)} \ln(\lambda_{BLV}/\lambda_u)^{-2(2+\epsilon)/(3+2\epsilon)}}{(1/\ln(\lambda_{BLV}) + 1/f)^{-4\delta(\epsilon)/(3+2\epsilon)}}.\quad (20)$$

For $\epsilon = 0$ (corresponding to low Prandtl number), we obtain a regime $Nu = Ra^{1/3}$ with logarithmic corrections which depend on the Rayleigh number: for low Rayleigh number, the scaling of the boundary layer is determined by the logarithmic region, making $Nu \sim Ra^{1/3}/\ln(Ra)^{8/3}$. This regime mimics a scaling exponent close to 1/4 (see Figure 6). For larger Rayleigh numbers, the scaling of the boundary layer scale is determined by the bulk flow, changing the correction to $Nu \sim Ra^{1/3}/(\ln(Ra))^{4/3}$. This results in a larger effective exponent, of the order of 0.28. In this regime, the boundary layer scale like $\lambda_{BLV} \sim (Re \ln(Re))^{-1/2}$, providing an approximate power-law in Rayleigh with exponent -0.2 . All these features were observed in the mercury experiment of [27]. For $\epsilon = -1/2$ ($Pr > 0.35$, we obtain a regime in which the Nusselt depends only weakly on the Prandtl number $Nu \sim Ra^{1/2}/(\ln(Re))^{3/2}$. This regime corresponds to the "ultra-hard" convective regime predicted by Kraichnan [5], but with logarithmic corrections. In Fig. 7, we compare this regime with the $Nu \sim Pr^{0.072} Ra^{0.389}$ approximate power-law measured by Chavanne et al [28] in Helium, at $Ra > 10^{11}$. Our formula predicts a very weak dependence of in the Prandtl number, like in [28], but with opposite sign. This could be accounted for minute variations of the mean profile around the value $\epsilon = -1/2$. However, the plus sign of the fit by Chavanne et al. could be an artifact due to the scatter of the data. Indeed several measurements performed at fixed Rayleigh number and for increasing Prandtl show that Nu tends to decrease rather than increase, as in the formula by Chavanne et al. The predictions in this regime are also in agreement with their Reynolds number measurements $Re \sim Ra^{0.49} Pr^{-0.75}$ if one considers that this Reynolds number is based on the vertical velocity, i.e. $Re \sim w_c Pr$.

Interestingly enough, the slight discrepancy between our prediction for $d \ln w_c / d \ln Pr$ (little less than 0.25) and the Chavanne et al. fit (little more than 0.25) can be traced back to the discrepancy in the Nusselt number. So there must be some systematic error present at this level, either in the theory, or in the experiments. In any case, this new regime may explain to puzzling facts: 1) why Glazier et al do not observe transition towards a new scaling regime, despite their very large Reynolds number. This is because they were already in the ultra-hard regime! 2) why for the same geometry and the same aspect ratio, Niemela et al did not observe a transition towards the regime observed by Chavanne et al. It is because, somehow, they do not allow the temperature fluctuations to grow enough so that their contribution supersedes that of the mean flow.

A good summary of our results can be found in the tables. For completeness, we have indicated the scaling behavior of various quantities measured in experiments, like Δ_c or w_c (the value of temperature or velocity fluctuations at the center of the cell). These values can be estimated from (9), with $z = 1$. When available, we have indicated comparison with measurements. This summary shows that many scaling behaviors observed in recent experiments can be reproduced using log-corrected scaling laws. Overall, the agreement of the theory based our toy model of thermal convection is excellent for the case $Pr \sim 1$ (Helium). It predicts reasonably well the Rayleigh dependence of the quantities for low Prandtl number, but it is not clear whether the Prandtl number dependence in these regimes is well predicted. This might be caused by our initial hypothesis (taking $Pr^t = 1$). Also, we were unsure where to put in this picture the recent experiments by [8] performed in water. The difficulty is that these experiments are performed at many different aspect ratio, and it is difficult to disentangle the aspect ratio dependence of the local scaling exponents with other dependences. At least in the case of Helium, apparently, we reached a point where experimental measurements cannot discriminate between logarithmic corrections to scaling, or corrections due to superposition of power laws, like proposed by [6]. This calls for identification of more stringent tests of theories. One possibility, which has been so far under-exploited, would be to concentrate on statistical properties rather than average, i.e. on probability distributions functions. In this context, it is interesting to note that our toy model of turbulent convection allows such investigations, via a Langevin formalism exploiting the linearity and the stochasticity of the equations. In neutral condition, our toy model leads to PDF's for velocity with qualitatively similar behavior than the PDF's measured in high Reynolds number flows [29]. The generalization of these results to the convective regime is underway.

I thank the Fluid Mechanics group of the ENS Lyon for many very interesting discussions. My special thanks goes to B. Castaing for his continuous interest and support in the present work.

TABLES

Q(X,Y)	This theory		Experiments	
	$d \ln Q/dX$	$d \ln Q/dY$	$d \ln Q/dX$	$d \ln Q/dY$
Nu	1/4	-1/12		
$Re = u_\tau/Pr$	3/8	-5/8		
Δ_c	-3/16	-13/48		
w_c	7/16	3/16		
λ_{BLT}	-1/4	1/12		
λ_{BLV}	-1/4	5/12		

TABLE I. Summary of local exponents of different physical quantities in regime 1: low Reynolds number, mean flow dominates. In this table $X = \ln Ra$ and $Y = \ln Pr$. No dependence on X or Y of the scaling exponent indicates real scaling with respect to Ra or Pr respectively.

Q(X,Y)	This theory		Experiments	
	$d \ln Q/dX$	$d \ln Q/dY$	$d \ln Q/dX$	$d \ln Q/dY$
Nu	2/7	-1/7	0.282	
$Re = u_\tau/Pr$	3/7	-5/7	0.43	
Δ_c	-5/28	-2/7	-0.147	
w_c	13/28	1/7	0.491	
λ_{BLT}	2/7	-1/7		
λ_{BLV}	np	np		

TABLE II. Summary of local exponents of different physical quantities in regime 2: $Pr > 0.35$, mean flow dominates. This regime corresponds to the theory of [4]. The measurements are those of the Chicago group [3]. However, this experiments might well be better described by regime 4, see below. In this table $X = \ln Ra$ and $Y = \ln Pr$. No dependence on X or Y of the scaling exponent indicates real scaling with respect to Ra or Pr respectively. The symbol np means not predicted by this theory.

Q(X,Y)	This theory		Experiments	
	$d \ln Q/dX$	$d \ln Q/dY$	$d \ln Q/dX$	$d \ln Q/dY$
Nu	$1/5 + 3f/5(fX + X^2)$	$1/5 + 3f/5(fY + Y^2)$	0.26 then 0.2	0.21
$Re = u_\tau/Pr$	$2/5 + f/5(fX + X^2)$	$-3/5 + f/5(fY + Y^2)$	0.424	
Δ_c	$-1/5 + 3f/20(fX + X^2)$	$-1/5 + 3f/20(fY + Y^2)$		
w_c	$2/5 + 9f/20(fX + X^2)$	$2/5 + 9f/20(fY + Y^2)$		
λ_{BLT}	$-1/5 - 3f/5(fX + X^2)$	$-1/5 - 3f/5(fY + Y^2)$		
λ_{BLV}	np	np		

TABLE III. Summary of local exponents of different physical quantities in regime 3: $Pr < 0.35$, mean flow dominates. The measurements are from [2]. In this table $X = \ln Ra$ and $Y = \ln Pr$ and f is a constant, depending on the shape of the bulk velocity profile. This constant is not predicted by the theory. No dependence on X or Y of the scaling exponent indicates real scaling with respect to Ra or Pr respectively. The symbol np means not predicted by this theory.

Q(X,Y)	This theory		Experiments	
	$d \ln Q/dX$	$d \ln Q/dY$	$d \ln Q/dX$	$d \ln Q/dY$
Nu	$1/3 - 2/(3X)$	$-1/9 - 2/3Y$	0.309^1	-0.2^2
$Re = u_\tau/Pr$	$1/2 - 1/X$	$-2/3 - 1/Y$	$0.43^{2,3}$	-0.75^2
Δ_c	$-1/6 - 1/6X$	$-5/18 - 1/6Y$	-0.145^1	
w_c	$1/2 - 1/2X$	$1/6 - 1/2Y$	0.53^4	0.08^4
λ_{BLT}	$-1/3 + 2/3X$	$1/9 + 2/3Y$	-0.28^3	
λ_{BLV}	$-1/6 + 1/3X$	$1/9 + 1/3Y$	-0.14^3	0.21^3

TABLE IV. Summary of local exponents of different physical quantities in regime 4: $Pr > 0.35$, fluctuations dominates. The measurements are from [2] (superscript 1), [26] (superscript 2), [20] (superscript 3) and [18] (superscript 4). In this table $X = \ln Ra$ and $Y = \ln Pr$. No dependence on X or Y of the scaling exponent indicates real scaling with respect to Ra or Pr respectively. The symbol np means not predicted by this theory.

Q(X,Y)	This theory		Experiments	
	$d \ln Q/dX$	$d \ln Q/dY$	$d \ln Q/dX$	$d \ln Q/dY$
Nu	$1/3 - 4/3X - 4f/3(fX + X^2)$	$1/3 - 4/(3Y) - 4f/3(fY + Y^2)$	0.25 then 0.285	
$Re = u_\tau/Pr$	$1/3 - 1/3X - f/3(fX + X^2)$	$-2/3 - 1/3Y - f/3(fY + Y^2)$		
Δ_c	$-1/6 - 1/3X - f/3(fX + X^2)$	$-1/6 - 1/3Y - f/3(fY + Y^2)$		
w_c	$1/2 - 1/3X - f/3(fX + X^2)$	$1/2 - 1/3Y - f/3(fY + Y^2)$		
λ_{BLT}	np	np		
λ_{BLV}	$-1/6 + 1/6X + f/6(fX + X^2)$	$-1/6 + 1/6Y + f/6(fY + Y^2)$	-0.2	

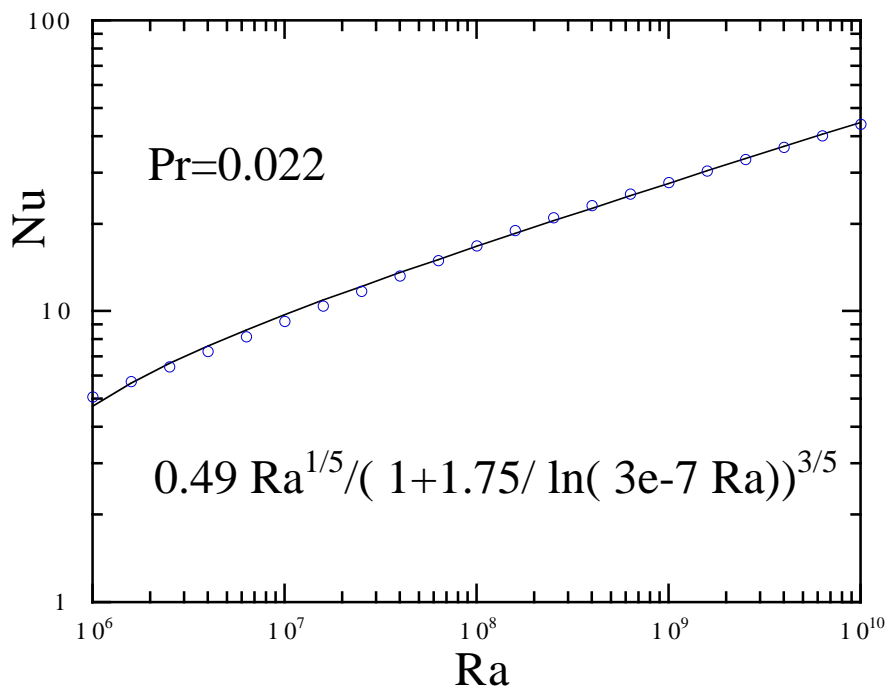
TABLE V. Summary of local exponents of different physical quantities in regime 5: $Pr < 0.35$, fluctuations dominates and $\lambda_\theta \gg \lambda_u$. The measurements from [27]. In this table $X = \ln Ra$ and $Y = \ln Pr$ and f is a constant, depending on the shape of the bulk velocity profile. This constant is not predicted by the theory. No dependence on X or Y of the scaling exponent indicates real scaling with respect to Ra or Pr respectively. The symbol np means not predicted by this theory.

Q(X,Y)	This theory		Experiments	
	$d \ln Q/dX$	$d \ln Q/dY$	$d \ln Q/dX$	$d \ln Q/dY$
Nu	$1/2 - 3/(2X)$	$-3/2Y$	0.389	0.072
$Re = u_\tau/Pr$	$3/8 - 3/8X$	$-3/4 - 3/8Y$		
Δ_c	$-1/8 - 3/(8X)$	$-1/4 - 3/8Y$		
w_c	$5/8 - 9/8X$	$1/4 - 9/8Y$	0.49	0.28
λ_{BLT}	np	np		
λ_{BLV}	$-1/8 + 1/8X$	$1/4 + 1/4Y$		

TABLE VI. Summary of local exponents of different physical quantities in regime 6: $Pr > 0.35$, fluctuations dominates and $\lambda_\theta \gg \lambda_u$. The measurements are from [28]. In this table $X = \ln Ra$ and $Y = \ln Pr$. No dependence on X or Y of the scaling exponent indicates real scaling with respect to Ra or Pr respectively. The symbol np means not predicted by this theory.

REFERENCES

- [1] R.J. Goldstein, H.D. Chiang and D.L. See, *J. Fluid Mech.* **213**, 111 (1990)
- [2] S. Cioni, S. Ciliberto and J. Sommeria *J. Fluid Mech.* **335** 111 (1997)
- [3] B. Castaing, G. Gunaratne, F. Heslot, L. Kadanoff, A. Libchaber, S. Thomae, X-Z. Wu, S. Zaleski and G. Zanetti *J. Fluid Mech.* **204** 1 (1989).
- [4] B. I. Shraiman and E.D. Siggia *Phys. Rev. A.* **42**, 3650 (1990).
- [5] R. Kraichnan *Phys. Fluids* **5** 1374 (1962)
- [6] S. Grossmann and D. Lohse *J. Fluid Mech.* **407** 27 (2000).
- [7] S. Grossman and D. Lohse preprint (2000).
- [8] X. Xu, K.M.S. Bajaj and G. Ahlers, *Phys. Rev. Letter*, **84**, 4357 (2000).
- [9] W.V.R. Malkus *Proc. Roy. Soc. London., A* **225**, 185-195. (1954); W.V.R. Malkus *Proc. Roy. Soc. London., A* **225**, 195-212. (1954)
- [10] F.H. Busse *Rep. Prog. Phys.* **41** 1930 (1978).
- [11] J.J. Niemela, L. Skrbek, K.R. Sreenivasan and R.J. Donnelly *Nature* **404** 837 (2000).
- [12] B. Dubrulle, J-P. Laval and P. Sullivan preprint available at <http://webast.ast.obs-mip.fr/people/bdubru>. (2000).
- [13] B. Dubrulle, *Europhys. Letters* **51** 513 (2000).
- [14] B. Dubrulle, J-P. Laval, P. Sullivan and J. Werne A dynamical subgrid scale model for the planetary surface layer 1. The model *submitted to J. Atmosph. Sci.* (2000).
- [15] J. Werne, *Phys. Rev. E* **48** 1020-1035 (1993).
- [16] S. Nazarenko *Phys. Lett. A* **264** 444 (2000); S. Nazarenko, N. Kevlahan and B. Dubrulle *Physica D* **139** 158 (2000); B. Dubrulle, J-P. Laval, S. Nazarenko and N. Kevlahan preprint.
- [17] T. Segawa, A. Naert and M. Sano, *Phys. Rev. E* **57** 557 (2008); A. Naert, T. Segawa and M. Sano *Phys. Rev. E* **56** R1302 (1997).
- [18] R. Verzicco and R. Camussi *J. Fluid Mech.* **383** 55 (1999)
- [19] R.M. Kerr, *J. Fluid Mech.* **310** 139 (1996).
- [20] R. M. Kerr and J. R. Herring (2000) preprint.
- [21] R.M. Kerr, private communication (1999).
- [22] J. Werne, private communication; K. Julien, S. Legg, J. Mc Williams and J. Werne, *J. Fluid Mech.* **322** 243 (1996).
- [23] S. Ciliberto and C. Laroche *Phys. Rev. Letters* **82** 3998 (1999).
- [24] S. Ciliberto, S. Cioni and C. Laroche *Phys. Rev E* **54** R5901 (1996).
- [25] T. Takeshita, T. Segawa, J.A. Glazier and M. Sano *Phys. Rev. Letter* **76** 1465 (1996).
- [26] S. Ashkenazi and V. Steinberg *Phys. Rev. Letter* **83**, 3641 (1999).
- [27] J.A. Glazier, T. Segawa, A. Naert and M. Sano, *Nature* **398** 307 (1999).
- [28] X. Chavanne, F. Chilla, B. Castaing, B. Hébral, B. Chabaud and J. Chaussy, *Phys. Rev. Letters* **79**, 3648 (1997).
- [29] J-P. Laval, B. Dubrulle and S. Nazarenko Non-locality and intermittency in 3D turbulence *submitted to Phys. Fluids* (2000).



FIGURES

FIG. 1. Nusselt vs Rayleigh in regime 3 ($Pr < 0.35$, mean flow dominates). The symbols are the power-law fits of the experimental measurements by [2]. The line is the theoretical formula predicted by the toy model (eq. (16) with $\epsilon = 0$).

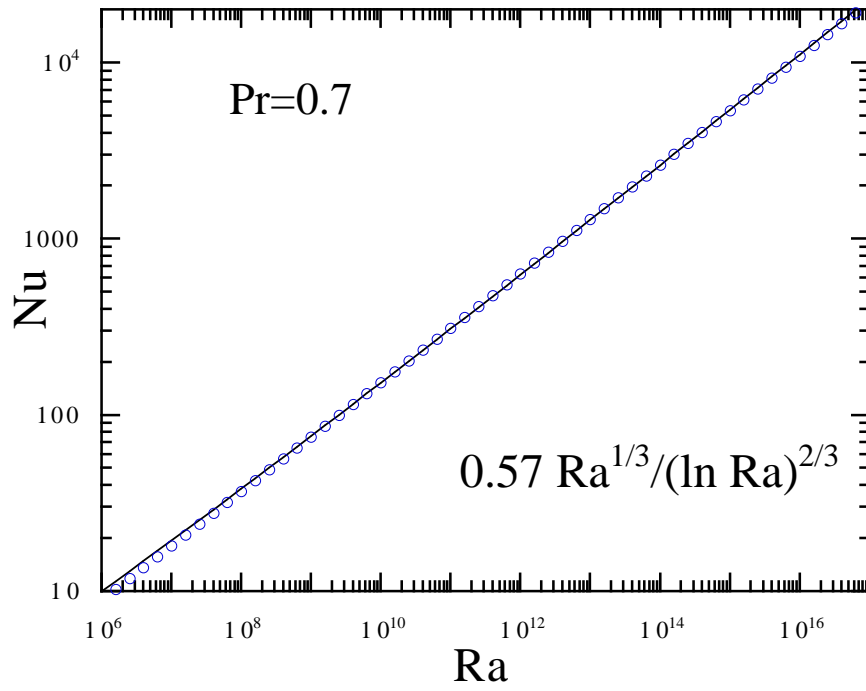


FIG. 2. Nusselt vs Rayleigh in regime 4 ($Pr > 0.35$, velocity fluctuations dominate but temperature fluctuations are negligible). The symbols are the power-law fit $Nu \sim Ra^{0.309}$ of the experimental measurements by [11]. The line is the theoretical formula predicted by the toy model (eq. (17) with $\epsilon = -1/2$).

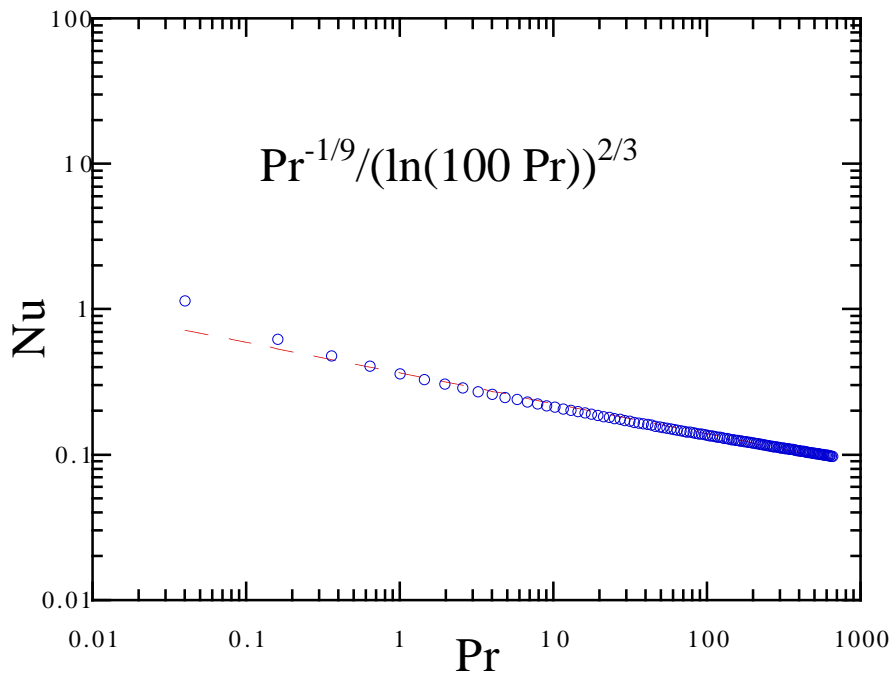


FIG. 3. Nusselt vs Prandtl in regime 4 ($Pr > 0.35$, velocity fluctuations dominate but temperature fluctuations are negligible). The symbols is the theoretical formula (eq. (17) with $\epsilon = -1/2$). The dotted line is a power-law fit, with slope -0.2 , mimicking the experimental fit of [26].

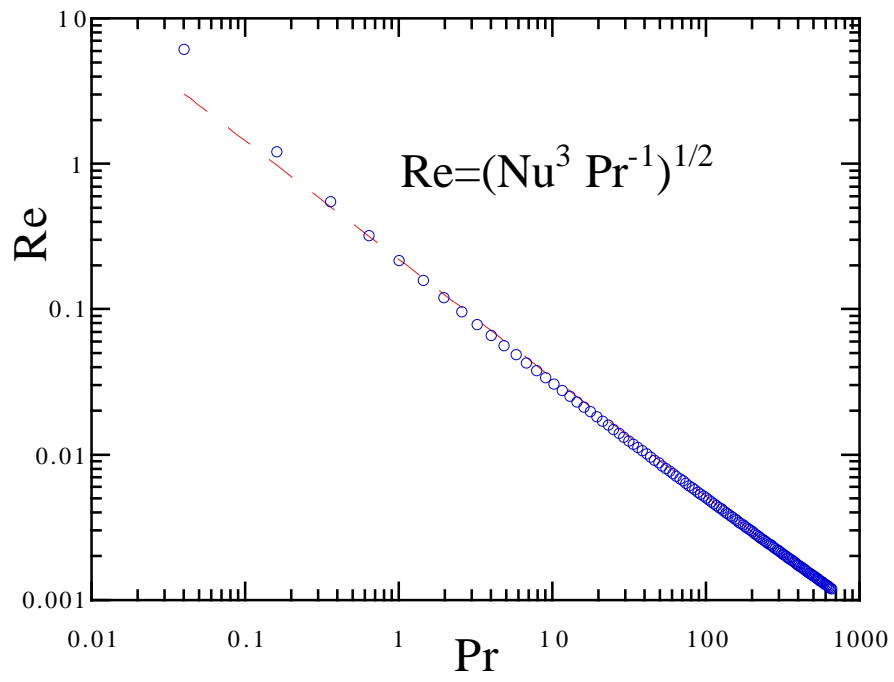


FIG. 4. Reynolds vs Prandtl in regime 4 ($Pr > 0.35$, velocity fluctuations dominate but temperature fluctuations are negligible). The symbols is the theoretical formula. The dotted line is a power-law fit, with slope -0.8 , mimicking the experimental fit of [26].

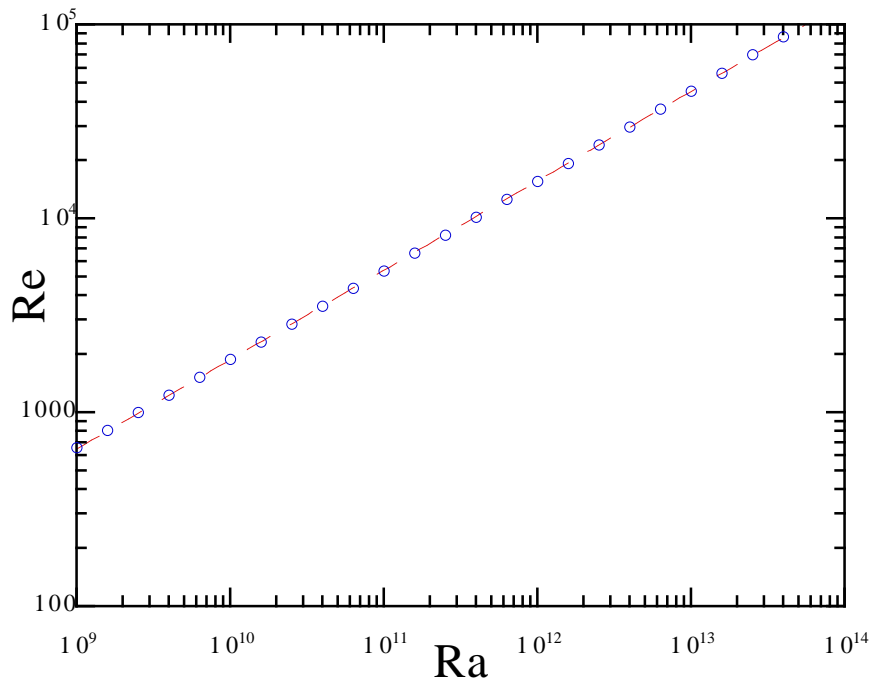


FIG. 5. Reynolds vs Rayleigh in regime 4 ($Pr > 0.35$, velocity fluctuations dominate but temperature fluctuations are negligible). The symbols is the theoretical formula. The dotted line is a power-law fit, with slope 0.43, mimicking the experimental fit of [26].

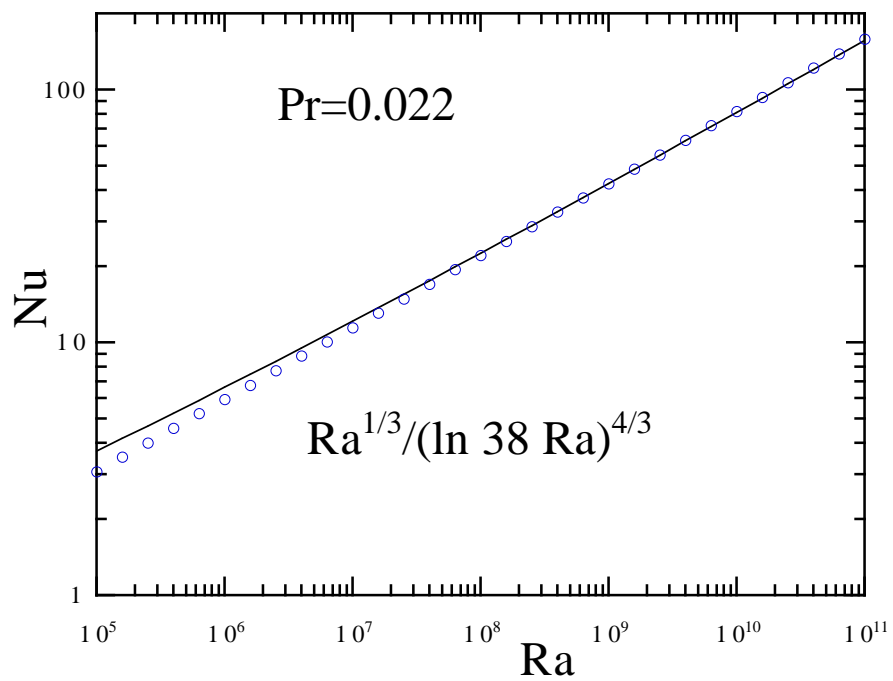


FIG. 6. Nusselt vs Rayleigh in regime 5 ($Pr < 0.35$, fluctuations dominates). The symbols are the power-law fits of experimental measurements by [27]. The line is the theoretical formula predicted by the toy model (eq. (20) with $\epsilon = 0$).

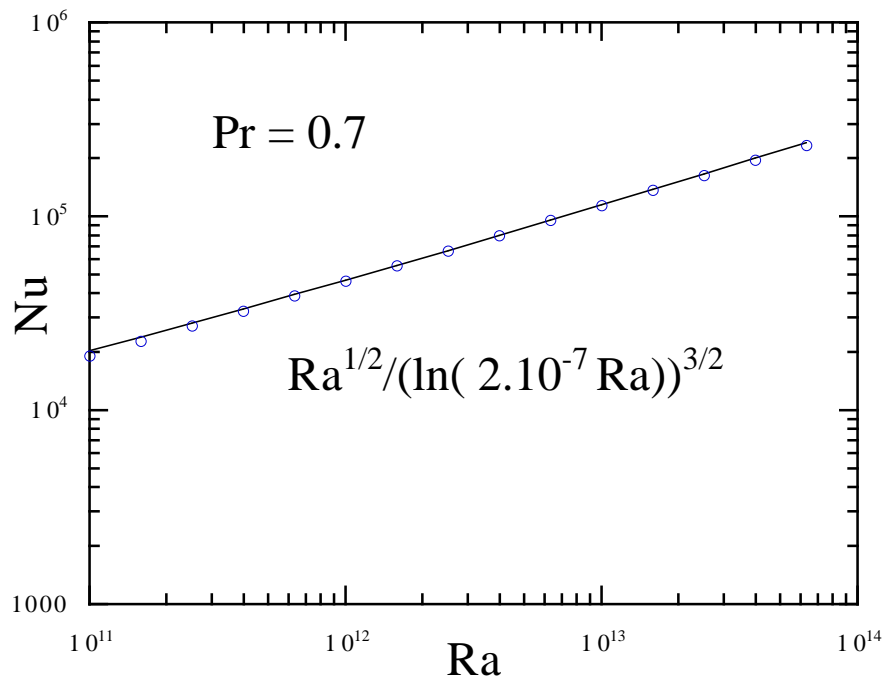


FIG. 7. Nusselt vs Rayleigh in regime 6 ($Pr > 0.35$, fluctuations dominates. The symbols are the power-law fits of the experimental measurements by [28]. The line is the theoretical formula predicted by the toy model (eq. (20) with $\epsilon = -1/2$).